Data-Driven Adaptive Predictive Frequency Control for Power Systems with Unknown and Time-Varying Inertia

Yunzheng Zhao[1,2], Tao Liu[1,2]
[1] Department of Electrical and Electronic Engineering
The University of Hong Kong
Hong Kong, China
[2] HKU Shenzhen Institute of Research and Innovation
Shenzhen, China
{zhaoyz,taoliu}@eee.hku.hk

David J. Hill
Department of Electrical and Computer Systems Engineering
Monash University
Melbourne, Australia
davidj.hill@monash.edu

***Abstract*—This paper proposes a novel data-based adaptive predictive frequency control method for multi-area power systems with unknown and time-varying inertia. Firstly, a data-based representation is built and updated at each instant based on behavioural system theory by using historical input-output data, where a moving horizon estimation method is used to deal with the unknown time-varying inertia issue adaptively. Then, the optimal frequency control signal is computed by solving an optimization problem under the framework of data-based predictive control. Simulation results on a power system with three control areas demonstrate the effectiveness of the proposed method.**

***Index Terms*—Data-driven adaptive predictive frequency control, time-varying inertia, behavioural system theory, moving horizon estimation.**

I. Introduction

Load frequency control (LFC) is aimed to maintain the frequency of a power system with multiple control areas at its nominal value (50 Hz or 60 Hz) and the tie-line powers between connected areas at their scheduled values [1]. Traditionally, automatic generation control (AGC) is used to achieve these two objectives. But the increasing penetration of renewables in terms of converter-interfaced generators (CIGs) poses new challenges to power system frequency control. For one thing, the intermittence and limited predictability of renewables limit the control capability of AGC. For another thing, CIGs usually do not provide inertia to power systems [2]. As more synchronous generators are replaced with CIGs, the system inertia reduces dramatically and even becomes time-varying, which makes the system more fragile to disturbances and hard to control [3].

Submitted to the 23rd Power Systems Computation Conference (PSCC 2024). This work was supported by the Research Grants Council of the Hong Kong Special Administrative Region under the Early Career Scheme through Project No. 27206021 and the National Natural Science Foundation of China through Project No. 62173287. (*corresponding author: Tao Liu*)

Model predictive control (MPC) offers a possible solution to deal with the fast fluctuations of renewable generation outputs [4]. It calculates a sequence of optimal control signals at each sampling instant by solving an optimization problem over a receding finite time horizon, in which various constraints are considered. Then, usually only the first step of the obtained control sequence is used to control the system. The process is repeated at next sampling instant. Uncertainties of renewables are handled in this receding horizon control (RHC) framework. However, MPC strongly depends on the system model, which is usually costly and even hard to be obtained. Many MPC-based LFC methods do not consider the time-varying inertia caused by CIGs and use a fixed system model, which may degenerate the control performance and even cause stability issues.

To improve the LFC performance under time-varying inertia, a modulated power balance control loop is developed to augment AGC in [5]. In all scenarios under different inertias, the proposed method exhibits better frequency regulation performance than AGC with reduced frequency oscillations and overshoots. In [6], a controller depending on the derivative of the frequency is used as a virtual inertia resource to combine with the linear-quadratic regulator controller to stabilize the system when the inertia decreases rapidly. These works only focus on stabilization of the systems with time-varying inertia, and their control signals may be suboptimal.

In view of the aforementioned issues, we propose a data-driven adaptive predictive frequency control (DAPFC) approach. The basic idea is to solve a RHC optimization problem to get the control signals based on a data-based system representation, which is updated at each sampling instant to allow for the power system having time-varying inertia. To build and adaptively update the data-based system representation, the behavioural system theory [7] and moving horizon estimation (MHE) scheme [8] are adopted, where the discrepancy between the latest measurement trajectories of input-output (IO) data and those generated by the data-

based system representation is minimized. Then, the optimal frequency control signal is calculated by solving a quadratic programming (QP) problem under the framework of data-based predictive control. Simulation results on a power system with three control areas demonstrate the effectiveness of the proposed method.

In the rest of this paper, Section II presents the problem formulation. Section III proposes the DAPFC method. Section IV shows the case study and Section V gives the conclusion.

Notation: Let $\mathbb{R}_{\geq 0}$, $\mathbb{R}_{>0}$, $\mathbb{R}^m$ and $\mathbb{R}^{m\times n}$ represent the set of non-negative real numbers, positive real numbers, m-dimensional real column vectors, and $(m \times n)$-dimensional real matrices, respectively. Denote $\mathbb{N}^+$ as the set of positive integers. For a set of vectors $u_1, u_2, \ldots, u_n$, let $\text{col}(u_1, u_2, \ldots, u_n) := (u_1^\top, u_2^\top, \ldots, u_n^\top)^\top$. For a matrix A, $A^\dagger$ denotes its Moore-Penrose inverse. Let $\mathbb{0}_{m\times n}$ denote the $(m \times n)$-dimensional zero matrix and I_m denote the m-dimensional identity matrix. Let $|p|$ denote the absolute value of scalar p. The notation $\|x\|_Q$ denotes the quadratic form $x^\top Qx$ where $x \in \mathbb{R}^m$ is a vector and $Q \in \mathbb{R}^{m\times m}$ is a weight matrix.

II. Problem Formulation

Consider a power transmission system with N control areas. Each control area i, $i \in \mathcal{N} = \{1, \ldots, N\}$, is represented by an equivalent generating unit [18], and the following widely adopted assumptions [9] for frequency control of transmission systems are made:

1) The power network is connected and the transmission lines are lossless.
2) The frequency of the power system is mainly affected by active power flows.
3) Bus voltage magnitudes are fixed.

Under these assumptions, we study the LFC problem of the N-control-area power system with time-varying net loads, i.e., the load consumption minus power generation of renewables. The nonlinear power system is assumed to initially operate at an equilibrium point. If the perfect system model is accessible, MPC can be adopted for LFC [4]. Specifically, the nonlinear power system is usually linearized at the initial operating point, and then the linearized model is discretized with a sampling period $T_s \in \mathbb{R}_{>0}$ to obtain a discrete-time linear prediction model. A QP problem is formulated based on the prediction model to calculate the optimal control signals. Nevertheless, perfect model information is in general costly or even hard to be obtained. To solve this issue, in this paper we concentrate on developing a data-driven predictive control method.

We assume that there is a control center above all control areas and it can access the IO data of the whole system. The input and output signals of the system at sampling instant k are denoted by

$$u(k) = \text{col}(u_1(k), \ldots, u_N(k)) \in \mathbb{R}^m \tag{1a}$$
$$y(k) = \text{col}(y_1(k), \ldots, y_N(k)) \in \mathbb{R}^p \tag{1b}$$

where p, m refer to the dimensions of output and input signals, respectively, and the input $u_i(k)$ and output $y_i(k)$ of area i, $i \in \mathcal{N}$, are

$$u_i(k) = (p_{ci}(k), p_{di}(k))^\top \tag{2a}$$
$$y_i(k) = (\delta_i(k), \omega_i(k))^\top \tag{2b}$$

with $p_{ci}(k)$ and $p_{di}(k)$ being the control input, i.e., generation command and the external input, i.e., net load, respectively; $\delta_i(k)$ and $\omega_i(k)$ being the power angle with respect to the synchronously rotating reference and frequency deviation from the nominal value. As mentioned previously, the control targets are twofold. First, it is to regulate the frequency at its nominal value, i.e., $\omega_i(k) = 0$. Second, it is to maintain the tie-line powers between connected areas at their scheduled value, i.e., $p_{tie-ij}(k) = p^0_{tie-ij}$, where $j \in \mathcal{N}_i$ with $\mathcal{N}_i$ being the index set of areas directly connected to area i, p^0_{tie-ij} is the scheduled tie-line power between area i and j, and

$$p_{tie-ij}(k) = B_{ij} \sin(\delta_i(k) - \delta_j(k)) \tag{3}$$

where the coefficient B_{ij} is defined as $B_{ij} = |V_i||V_j|Y_{ij}$ with $|V_i|$, $|V_j|$ being the voltage magnitudes of areas i and j, Y_{ij} being the susceptance of branch (i, j). To control the tie-line powers, we regulate the power angle difference $\delta_{ij}(k)$ to δ^0_{ij} with $\delta_{ij}(k) = \delta_i(k) - \delta_j(k)$ and δ^0_{ij} being the value of $\delta_{ij}(k)$ at the initial operating point.

High shares of CIGs entering the dispatch process reduces the aggregated rotational inertia. Moreover, the system inertia may even become time-varying due to the intermittent penetration of renewables, which causes the aggregated system inertia costly to be estimated in real-time. Under this new scenario, the power system with low inertia may be unstable if it is controlled by traditional AGC [5]. In addition, the trajectories prediction of the conventional MPC with a fixed system model may not be accurate due to the time-varying inertia, which may deteriorate the LFC performance, and also the real-time inertia estimation is costly to achieve. To allow for this new scenario under time-varying and unknown inertia, we focus on designing an online adaptive LFC method.

III. Proposed Data-Driven Adaptive Predictive Frequency Control Method

In this section, we propose a novel DAPFC method which includes: offline data collection, online adaptive system representation, and online predictive control.

Consider a signal $x^d(k) \in \mathbb{R}^q$ with $q \in \mathbb{N}^+$ where the superscript d denotes that the data is collected offline. The matrix $x^d_{[k,k+T]} \in \mathbb{R}^{q\times(T+1)}$ with $T \in \mathbb{N}^+$ defined below refers to a sequence of $x^d(k)$ over the time period $[k, k+T]$

$$x^d_{[k,k+T]} = [x^d(k), \ldots, x^d(k+T)]. \tag{4}$$

The associated Hankel matrix for the signal sequence $x^d_{[0,T-1]}$ is defined as

$$\mathscr{H}_L(x^d_{[0,T-1]}) = \begin{bmatrix} x^d(0) & x^d(1) & \cdots & x^d(T-L) \\ x^d(1) & x^d(2) & \cdots & x^d(T-L+1) \\ \vdots & \vdots & \ddots & \vdots \\ x^d(L-1) & x^d(L) & \cdots & x^d(T-1) \end{bmatrix} \tag{5}$$

where $L \in \mathbb{N}^+$ with $L \leq T$ is the depth of the Hankel matrix. The input $x^d_{[0,T-1]}$ is persistently exciting (PE) of order L if the Hankel matrix $\mathscr{H}_L(x^d_{[0,T-1]})$ is of full row rank [10].

A. Offline data collection

In the offline process, we collect the IO data under 2^N extreme historical scenarios, where each scenario corresponds to one of the 2^N combinations of the N-area inertia at their maximum and minimum values, which are detailed as

$$\begin{aligned} H(k) &= [\underline{H_1}, \underline{H_2}, \ldots, \underline{H_N}]^\top \\ H(k) &= [\underline{H_1}, \overline{H_2}, \ldots, \underline{H_N}]^\top \\ &\vdots \\ H(k) &= [\overline{H_1}, \overline{H_2}, \ldots, \overline{H_N}]^\top \end{aligned} \tag{6}$$

where $H(k) \in \mathbb{R}^N$ is the set of inertia of all areas at instant k; $\overline{H_i}$ and $\underline{H_i}$ are the maximum and minimum of inertia of area i, respectively. Since the inertia is unknown, we collect the data when each area has the lowest and highest share of renewables to estimate these extreme scenarios.

Under each scenario s, $s \in \{1, \ldots, 2^N\}$, we collect IO data that is rich and long enough. From the perspective of behavioral system theory, the IO data should be collected with a PE input $u^d_{[0,T-1]}$ of order $(m+p)n+1$ where n is the system order that is assumed to be known [11].

Remark 1: A data informativity check should be conducted to ensure that the collected data meets the PE condition. If the data is not rich enough to meet the PE condition, we should re-collect the IO data.

With these precollected IO data, a data-based system representation for each of the abovementioned extreme scenarios can be built based on the following lemma.

Lemma 1 [11]: For the system with fixed inertia, if the pre-collected input $u^d_{[0,T-1]}$ is PE of order $4Nn+1$, then the input and output signal are governed by the data-based representation (7) where the state $\mathcal{X}(k)$ is defined as

$$\mathcal{X}(k) = \text{col}(y(k-n), \ldots, y(k-1), u(k-n), \ldots, u(k-1)) \tag{8}$$

and the system matrices $\mathcal{A}$ and $\mathcal{B}$ are constructed with historical IO data, i.e.,

$$\begin{bmatrix} \mathcal{A} & \mathcal{B} \end{bmatrix} = \mathcal{X}^d_{[1,T]} \begin{bmatrix} \mathcal{X}^d_{[0,T-1]} \\ u^d_{[0,T-1]} \end{bmatrix}^\dagger. \tag{9}$$

Therefore, 2^N matrix pairs $[\mathcal{A}_s \ \mathcal{B}_s], s \in \{1, \ldots, 2^N\}$, are built in the offline data collection phase.

B. Online adaptive system representation

Inspired by (7) for system with fixed inertia, in the online phase, we aim at building a new data-based representation (10) to describe the system with time-varying inertia. Different from the constant $\mathcal{A}$ in (7), the system matrix $\mathcal{A}(k)$ in (10) is time-varying, which is updated at each sampling instant. In this subsection, the real-time estimation of $\mathcal{A}(k)$ is presented.

Before proceeding, we define a varying parameter $\rho(k) = [\rho_1(k), \ldots, \rho_N(k)]^\top$ with $\rho_i(k) = \frac{1}{H_i(k)}$, $i \in \mathcal{N}$. It belongs to the polytope $\mathcal{P}$ defined by

$$\mathcal{P} = \{\rho(k) \in \mathbb{R}^N : R\rho(k) \leq Q\} \tag{11}$$

where

$$\begin{aligned} Q &= \left[\tfrac{1}{\underline{H_1}}, \ldots, \tfrac{1}{\underline{H_N}}, -\tfrac{1}{\overline{H_1}}, \ldots, -\tfrac{1}{\overline{H_N}}\right]^\top, \\ R &= \begin{bmatrix} I_N \\ -I_N \end{bmatrix}. \end{aligned} \tag{12}$$

The following discussion illustrates that the system matrix $\mathcal{A}(k)$ to be estimated is affine with respect to the varying parameter $\rho(k)$. It should be noted that this analysis is to derive the analytical expression of $\mathcal{A}(k)$ based on the system model that is assumed to be known. But the proposed online adaptive estimation of $\mathcal{A}(k)$ does not require the model information.

For simplicity, we analyse the case with a two-control-area aggregated system in [18], where each area is represented by a second-order equivalent generating unit. The N-control-area power system with higher order can be analysed in a similar

$$\mathcal{X}(k+1) = \underbrace{\left[\begin{array}{cccccccc} 0_{p\times p} & I_p & \cdots & 0_{p\times p} & 0_{p\times m} & 0_{p\times m} & \cdots & 0_{p\times m} \\ \vdots & \vdots & \ddots & \vdots & \vdots & \vdots & \ddots & \vdots \\ 0_{p\times p} & 0_{p\times p} & \cdots & I_p & 0_{p\times m} & 0_{p\times m} & \cdots & 0_{p\times m} \\ -A_n & -A_{n-1} & \cdots & -A_1 & B_n & B_{n-1} & \cdots & B_1 \\ \hline 0_{m\times p} & 0_{m\times p} & \cdots & 0_{m\times p} & 0_{m\times m} & I_m & \cdots & 0_{m\times m} \\ \vdots & \vdots & \ddots & \vdots & \vdots & \vdots & \ddots & \vdots \\ 0_{m\times p} & 0_{m\times p} & \cdots & 0_{m\times p} & 0_{m\times m} & 0_{m\times m} & \cdots & I_m \\ 0_{m\times p} & 0_{m\times p} & \cdots & 0_{m\times p} & 0_{m\times m} & 0_{m\times m} & \cdots & 0_{m\times m} \end{array}\right]}_{\mathcal{A}} \mathcal{X}(k) + \underbrace{\left[\begin{array}{c} 0_{p\times m} \\ \vdots \\ 0_{p\times m} \\ 0_{p\times m} \\ \hline 0_{m\times m} \\ \vdots \\ 0_{m\times m} \\ I_m \end{array}\right]}_{\mathcal{B}} u(k) \tag{7}$$

$$\mathcal{X}(k+1)=\underbrace{\left[\begin{array}{cccccccc} 0_{p\times p} & I_p & \cdots & 0_{p\times p} & 0_{p\times m} & 0_{p\times m} & \cdots & 0_{p\times m}\\ \vdots & \vdots & \ddots & \vdots & \vdots & \vdots & \ddots & \vdots\\ 0_{p\times p} & 0_{p\times p} & \cdots & I_p & 0_{p\times m} & 0_{p\times m} & \cdots & 0_{p\times m}\\ -A_n(k) & -A_{n-1}(k) & \cdots & -A_1(k) & B_n(k) & B_{n-1}(k) & \cdots & B_1(k)\\ \hline 0_{m\times p} & 0_{m\times p} & \cdots & 0_{m\times p} & 0_{m\times m} & I_m & \cdots & 0_{m\times m}\\ \vdots & \vdots & \ddots & \vdots & \vdots & \vdots & \ddots & \vdots\\ 0_{m\times p} & 0_{m\times p} & \cdots & 0_{m\times p} & 0_{m\times m} & 0_{m\times m} & \cdots & I_m\\ 0_{m\times p} & 0_{m\times p} & \cdots & 0_{m\times p} & 0_{m\times m} & 0_{m\times m} & \cdots & 0_{m\times m} \end{array}\right]}_{\mathcal{A}(k)}\mathcal{X}(k)+\underbrace{\left[\begin{array}{c} 0_{p\times m}\\ \vdots\\ 0_{p\times m}\\ 0_{p\times m}\\ \hline 0_{m\times m}\\ \vdots\\ 0_{m\times m}\\ I_m \end{array}\right]}_{\mathcal{B}}u(k) \tag{10}$$

$$\begin{aligned}&(z^4+(k_1\rho_1+k_2\rho_2)z^3+(k_3\rho_1+k_4\rho_2)z^2+(k_5\rho_1+k_6\rho_2)z+k_7\rho_1+k_8\rho_2)Y(z)=\\ &\left[\begin{array}{cccc} k_9\rho_1z^2+k_{10}\rho_1z+k_{11} & k_{12}\rho_1z^2+k_{13}\rho_1z+k_{14} & 0 & 0\\ k_{15}\rho_1z^3+k_{16}\rho_1z^2+k_{17}z & k_{18}\rho_1z^3+k_{19}\rho_1z^2+k_{20}z & 0 & 0\\ 0 & 0 & k_{21}\rho_2z^2+k_{22}\rho_2z & k_{23}\rho_2z^2+k_{24}\rho_2z\\ 0 & 0 & k_{25}\rho_2z^3+k_{26}\rho_2z^2+k_{27}\rho_2z & k_{28}\rho_2z^3+k_{29}\rho_2z^2+k_{30}\rho_2z \end{array}\right]U(z)\end{aligned} \tag{15}$$

way. The discrete-time state-space model that is obtained by the Euler discretization is

$$\begin{aligned} x(k+1)&=C(\rho(k))x(k)+D(\rho(k))u(k)\\ y(k)&=Ex(k)\end{aligned} \tag{13}$$

where $x(k)=[\delta_1(k),\omega_1(k),\delta_2(k),\omega_2(k)]^\top$; the IO signals $u(k)$ and $y(k)$ are defined in (1); and matrices $C(\rho(k))$, $D(\rho(k))$ and E are detailed in [13]. Then, the transfer function is written as

$$G(z)=E(zI-C(\rho(k)))^{-1}D(\rho(k)). \tag{14}$$

The sampling period T_s is assumed to be chosen around 0.5 s and $\rho_i(k)$ varies around 0.2 (the system inertia usually fluctuates around 5 [12]), thus the terms with $T_s^3\rho_1(k)\rho_2(k)$ in $G(z)$ are near 10^{-3}, which is close to zero. Omitting the terms with $T_s^3\rho_1(k)\rho_2(k)$, we can obtain an approximate formula (15), where $U(z)$ and $Y(z)$ are the Z-transform of $u(k)$ and $y(k)$, respectively; $\rho_i(k)$ is denoted by ρ_i for notational simplicity; and $k_1,\ldots,k_{30}$ are constants, which are not detailed due to the space limitation. Applying the inverse Z-transform on (15), we can obtain that the relation between the input $u(k)$ and output $y(k)$ obeys

$$y(k)=-\sum_{h=1}^{n}A_h(k)y(k-h)+\sum_{h=1}^{n}B_h(k)u(k-h) \tag{16}$$

where the matrices $A_h(k)$ and $B_h(k)$ with $h\in\{1,\ldots,n\}$ satisfy (17). It is seen that the system matrix $\mathcal{A}$ composed of $A_h(k)$ and $B_h(k)$ with $h\in\{1,\ldots,n\}$ in (10) is approximately affine with respect to the varying parameter $\rho(k)$. We further assume this condition is satisfied in power systems with more than two control areas and rigorous theoretical proof will be studied in future work.

Hence, the matrix $\mathcal{A}(k)$ varies inside a polytope Ω [14], [15], which is defined by a convex hull of 2^N matrices $\mathcal{A}_s$, $s\in\{1,\ldots,2^N\}$, i.e.,

$$\Omega=\text{Co}\{\mathcal{A}_1,\ldots,\mathcal{A}_{2^N}\} \tag{18}$$

where the notation $\text{Co}\{\cdot\}$ denotes a convex hull; the matrices $\mathcal{A}_s$ obtained in the offline process are the vertices of the convex hull Ω.

Remark 2: In the case study part, the proposed DAPFC method shows robustness to inexact vertices, i.e., the IO data is collected when the inertia is not exactly at its maximum or the minimum. This robustness ensures that the proposed DAPFC still exhibits satisfying performance in practice even with inexact vertices captured by the 2^N data-based representations.

As the matrix $\mathcal{A}(k)$ varies inside a polytope Ω, it can be estimated as a convex combination of the vertices as follows

$$\mathcal{A}_{est}(k)=\sum_{s=1}^{s=2^N}\mu_s(k)\mathcal{A}_s \tag{19}$$

where $\mu_s(k)\in\mathbb{R}_{\geq 0}$ is the combination factor to be calculated. The set of the combination factors denoted by

$$\mu(k)=[\mu_1(k),\ldots,\mu_{2^N}(k)]^\top\in\mathbb{R}^{2^N} \tag{20}$$

belongs to a probability simplex defined as

$$\{\mu(k)|\sum_{s=1}^{s=2^N}\mu_s(k)=1,\mu_s(k)\geq 0\}. \tag{21}$$

At each time k, $\mathcal{A}(k)$ is updated by calculating the combination factor $\mu(k)$. To achieve this goal, we leverage the MHE idea in [16] and extend it to a data-driven fashion. The MHE scheme aims at minimizing the discrepancy between the latest measurement IO data trajectories and those generated by the

$$A_1(k)=\begin{bmatrix} k_1\rho_1+k_2\rho_2 & 0 & 0 & 0 \\ 0 & k_1\rho_1+k_2\rho_2 & 0 & 0 \\ 0 & 0 & k_1\rho_1+k_2\rho_2 & 0 \\ 0 & 0 & 0 & k_1\rho_1+k_2\rho_2 \end{bmatrix}, A_2(k)=\begin{bmatrix} k_3\rho_1+k_4\rho_2 & 0 & 0 & 0 \\ 0 & k_3\rho_1+k_4\rho_2 & 0 & 0 \\ 0 & 0 & k_3\rho_1+k_4\rho_2 & 0 \\ 0 & 0 & 0 & k_3\rho_1+k_4\rho_2 \end{bmatrix},$$
$$A_3(k)=\begin{bmatrix} k_5\rho_1+k_6\rho_2 & 0 & 0 & 0 \\ 0 & k_5\rho_1+k_6\rho_2 & 0 & 0 \\ 0 & 0 & k_5\rho_1+k_6\rho_2 & 0 \\ 0 & 0 & 0 & k_5\rho_1+k_6\rho_2 \end{bmatrix}, A_4(k)=\begin{bmatrix} k_7\rho_1+k_8\rho_2 & 0 & 0 & 0 \\ 0 & k_7\rho_1+k_8\rho_2 & 0 & 0 \\ 0 & 0 & k_7\rho_1+k_8\rho_2 & 0 \\ 0 & 0 & 0 & k_7\rho_1+k_8\rho_2 \end{bmatrix},$$
$$B_1(k)=\begin{bmatrix} 0 & 0 & 0 & 0 \\ k_{15}\rho_1 & k_{18}\rho_1 & 0 & 0 \\ 0 & 0 & 0 & 0 \\ 0 & 0 & k_{25}\rho_2 & k_{28}\rho_2 \end{bmatrix}, B_2(k)=\begin{bmatrix} k_9\rho_1 & k_{12}\rho_1 & 0 & 0 \\ k_{16}\rho_1 & k_{19}\rho_1 & 0 & 0 \\ 0 & 0 & k_{21}\rho_2 & k_{23}\rho_2 \\ 0 & 0 & k_{26}\rho_2 & k_{29}\rho_2 \end{bmatrix},$$
$$B_3(k)=\begin{bmatrix} k_{10}\rho_1 & k_{13}\rho_1 & 0 & 0 \\ k_{17} & k_{20} & 0 & 0 \\ 0 & 0 & k_{22}\rho_2 & k_{24}\rho_2 \\ 0 & 0 & k_{27}\rho_2 & k_{30}\rho_2 \end{bmatrix}, B_4(k)=\begin{bmatrix} k_{11} & k_{14} & 0 & 0 \\ 0 & 0 & 0 & 0 \\ 0 & 0 & 0 & 0 \\ 0 & 0 & 0 & 0 \end{bmatrix}, \tag{17}$$

data-based representation (10). Specifically, the following QP is solved to calculate $\mu(k)$

$$\begin{aligned} \min_{\mu(k)} \ & \sum_{l=k-N_b}^{k-1} (\|e(l)\|_{Q_e} + \|v(k)\|_{Q_v}) \\ \text{s.t. } & e(l+1) = \mathcal{X}(l+1) - \mathcal{X}_{est}(l+1), \\ & \mathcal{X}_{est}(l+1) = \mathcal{A}_{est}(k)\mathcal{X}(l) + \mathcal{B}u(l), \end{aligned} \tag{22}$$

where $v(k) = \mu(k) - \mu(k-1)$; $Q_e \in \mathbb{R}^{2Nn\times 2Nn}$ and $Q_v \in \mathbb{R}^{2^N\times 2^N}$ are two weight matrices; $N_b \in \mathbb{N}^+$ is the backward time horizon; $\mathcal{A}_{est}(k)$ is defined by (19). In the objective function, the minimization of $e(l)$ is to reduce the gap between IO trajectories generated by the estimated system representation and those of the real system over a backward horizon $[k-N_b, k-1]$; the penalty on $v(k)$ is to moderate the variance of $\mu(k)$ to avoid wildly fluctuating of the data-based representation as the system inertia is under slow change [17]. The weight assigned to $e(l)$ should be much larger than that to $v(k)$ as we mainly focus on getting a data-based system representation that is capable of best describing the power system dynamics.

Remark 3: The backward time horizon N_b is chosen experimentally. A trade-off between the complexity of the optimization problem and the accuracy of the data-based representation estimation should be considered in choosing N_b. For the three-control-area test system in the case study, we adopt $N_b = 3$.

C. Online predictive control

With the data-based system representation obtained in Section III-B, we conduct the online predictive control by solving the QP below at instant k to obtain the optimal control sequence

$$\begin{aligned} \min_{u(l)} \ & \sum_{l=k}^{k+N_f-1} (\sum_{i\in\mathcal{N}} (\|\omega_i(l)\|_{Q_\omega} + \sum_{j\in\mathcal{N}_i} \|\delta_i(l) - \delta_j(l)\|_{Q_\delta}) \\ & \qquad + \|u(l)\|_{Q_u}) \\ \text{s.t. } & \mathcal{X}(l+1) = \mathcal{A}_{est}(k)\mathcal{X}(l) + \mathcal{B}u(l), \\ & p_{ci_{\min}} \le p_{ci}(l) \le p_{ci_{\max}}, \quad i \in \mathcal{N}, \\ & p_{di}(l) = p_{di}^{\text{pre}}(l), \quad i \in \mathcal{N}, \end{aligned} \tag{23}$$

where $p_{ci_{\min}}$ and $p_{ci_{\max}}$ are the minimum and maximum control inputs of area i, respectively; $N_f \in \mathbb{N}^+$ is the prediction horizon; $p_{di}^{\text{pre}}(l)$ is the net load prediction obtained from the load and wind power forecasting system; Q_ω, Q_δ and Q_u are weighting matrices. For simplicity, we assume the data-based representation during the prediction horizon in (23) is unchanged to avoid heavy online computation burden.

After (23) is solved, we only adopt the first step of the obtained control sequence derived in (23) to control the power system. At next sampling instant $k+1$, the vector $\mathcal{X}(k)$ consisting of the latest IO data is updated and the system matrix $\mathcal{A}_{est}$ is reestimated. The aforementioned process of the proposed DAPFC algorithm is described in Figure 1.

Remark 4: The DAPFC needs to solve two optimization problems, i.e., (22) and (23), at each sampling instant. The computation time for each optimization problem on a laptop for the case study is milliseconds. Therefore, this algorithm can be solved in real time in actual systems.

IV. Case Study

In this section, we test the proposed DAPFC method on a power system with three connected areas. The diagram of the test system is shown in Figure 2. The system model and its parameters can be referred to in [18] and [19]. The scheduled tie-line powers between these connected areas are: $p_{tie-12} = 0.1$ p.u., $p_{tie-23} = -0.1$ p.u., $p_{tie-31} = 0$ p.u.. The maximum and minimum of the control signal are set as 4 p.u. and -4 p.u., respectively. The backward horizon N_b and forward horizon N_f are set as 3 and 15, respectively. The sampling period is set as 0.5 s. We use integral squared error

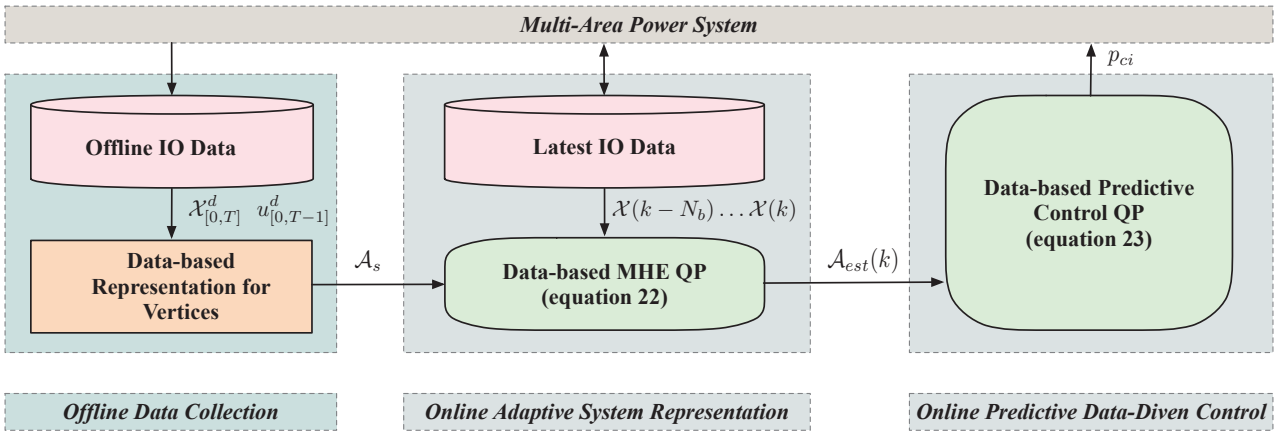

Fig. 1: Framework of the DAPFC Method.

(ISE) index J in [13] to measure the control performance, which is defined below

$$J = \int_0^t (\sum_{i=1}^{N}(\omega_i(t) + \sum_{j\in\mathcal{N}_i} \Delta p_{tie-ij}(t)))dt. \tag{24}$$

where $\Delta p_{tie-ij}(t) = p_{tie-ij}(t) - p^0_{tie-ij}$.

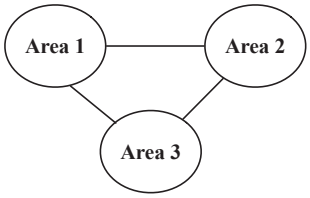

Fig. 2: Diagram of the three-area test system.

The rotational inertial profile of each area is shown in Figure 3. To simulate a range of scenarios in real power systems, we utilize various inertia profiles with distinct time-varying characteristics. For instance, when the penetration of renewables increases rapidly, the corresponding scenario involves a steep decline in the aggregated inertia. On the other hand, to imitate the intermittent integration of renewables, we use a scenario where the aggregated inertia declines slowly. Furthermore, when the penetration of renewables remains constant, aggregated inertia is maintained at a steady state. The minimum and maximum of the inertias are presented in Table I. Considering the data may be collected when the inertia may be not at its lower bound or upper bound, i.e., the vertices of the convex hull Ω in (18) can be inexact, we also collect a set of data by setting the inertia bounds of the simulation system different from but close to the real bounds in Table I to test the DAPFC method. It should be noted that the inexact inertia bounds are unknown in practice and we select a random set to collect data as shown in Table II.

The net load profile is presented in Figure 4. The forecasting horizon is 15 minutes. Based on the results in [20] and [21], we add a small noise on the net load prediction as the prediction error. The solid lines represent the predicted net load while the

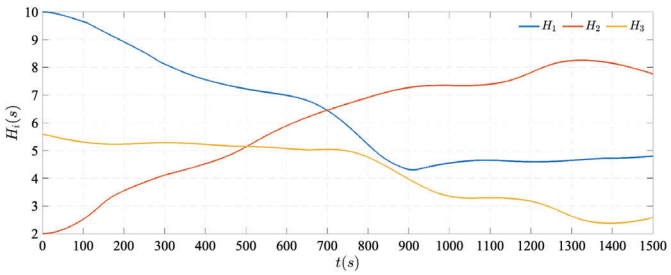

Fig. 3: Inertia profile of the three-area system.

dashed lines refer to the real net load. The control performance of the proposed method facing large prediction errors will be studied in future work.

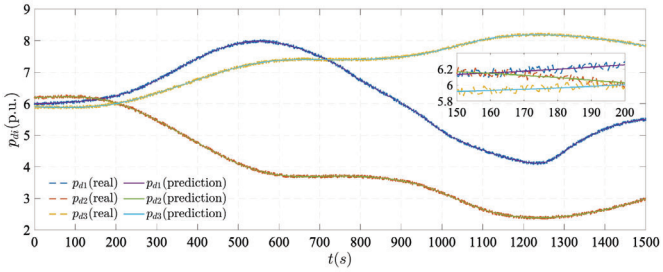

Fig. 4: Net load profile of the three-area system.

As there are three areas, the convex hull Ω in (18) has eight vertices. Therefore, we need to calculate eight combination factors, i.e., $\mu(k) = [\mu_1(k), \dots, \mu_8(k)]^\top$, to achieve online adaptive system representation. The initial value of $\mu(k)$ can be chosen randomly without impact on the effectiveness of the proposed DAPFC method. For simplicity, we initialize $\mu(0)$ as $\mu_1(0) = \mu_2(0) = \cdots = \mu_8(0) = 0.125$.

The control performance of the proposed method is compared with that of AGC, switching MPC with a time-varying exact system model (SMPC), and conventional MPC with a fixed system model (CMPC). For the CMPC, the inertias are set as $H_1 = 9, H_2 = 8, H_3 = 6$.

TABLE I: Minimum and maximum of the inertia of each area

	Area 1	Area 2	Area 3
$\underline{H_i}$	4	2	2
$\overline{H_i}$	10	9	6

TABLE II: Inexact minimum and maximum of the inertia of each area

	Area 1	Area 2	Area 3
$\underline{H_i}$	5	3	2
$\overline{H_i}$	10	8	5

Figure 5 depicts the frequency dynamics of three areas and the tie-line powers between these connected areas. Some partially enlarged pictures are added in Figure 5 to present the control performance of different methods more clearly. In order to display the control performance more comprehensively, we select different time periods to zoom in. Table III compares the ISE index of different control methods. As shown in these figures and Table III, with the proposed DAPFC method, the frequency deviation is regulated around zero and the tie-line powers are controlled around the scheduled value during the whole control process in both low-inertia and high-inertia scenarios. Furthermore, from these partially enlarged pictures, it can be found that the control performance of DAPFC is very close to that under SMPC with an accurate system model, which means that the proposed method is able to estimate and update the data-based system representation adaptively and accurately. While under AGC and CMPC with a fixed system model, all the frequency and tie-line powers fluctuate significantly. AGC does not take future net load predictions into consideration and the fixed AGC controller parameters setting may be not appropriate for a power system with time-varying inertia. CMPC calculates the control signal based on the fixed prediction model, which is inaccurate if the inertia varies. Therefore, the control performance is also poor.

As mentioned in Section III-B, the DAPFC algorithm with inexact vertices caused by data collection under scenarios when the inertia is not at its maximum or minimum is also tested in simulation. The frequency and tie-line power dynamics under DAPFC with inexact vertices is shown as the green dotted lines in Figure 5. It can be observed that the control performance is much better than those of AGC and CMPC, and close to that under DAPFC with exact vertices. Therefore, the proposed DAPFC method has robustness to the scenario under inexact vertices of the convex hull Ω in (18) caused by inaccurate offline data collection.

V. Conclusion

This paper have proposed a novel data-based adaptive predictive frequency control method for multi-area power systems with unknown and time-varying inertia. The proposed method consists of offline data collection, online data-based system representation, and online predictive control. In the offline process, historical input-output data has been collected under some extreme scenarios. In the online phase, a data-based system representation has been built and updated at each sampling instant based on the behavioural system theory and moving horizon estimation scheme. Then, the optimal frequency control signals have been calculated under the data-driven predictive control framework. Simulation results on a power system with three control areas have demonstrated the effectiveness of the proposed method.

References

[1] D. Jiao, C. Shao, B. Hu, K. Xie, C. Lin and Z. Ju, "Age-of-information-aware PI controller for load frequency control," *Protection and Control of Modern Power Systems*, vol. 8, no. 3, pp. 631-645, 2023.

[2] F. Milano, F. Dörfler, G. Hug, D. J. Hill and G. Verbič, "Foundations and challenges of low-inertia systems," *Power Syst. Computation Conf.*, Dublin, Ireland, 2018, pp. 1-25.

[3] A. Ulbig, T. Rinke, S. Chatzivasileiadis and G. Andersson, "Predictive control for real-time frequency regulation and rotational inertia provision in power systems," *IEEE Conf. Decis. Control*, Firenze, Italy, 2013, pp. 2946-2953.

[4] A. M. Ersdal, L. Imsland and K. Uhlen, "Model predictive load-frequency control," *IEEE Trans. Power Syst.*, vol. 31, no. 1, pp. 777-785, 2019.

[5] M. H. Syed, E. Guillo-Sansano, A. Mehrizi-Sani and G. M. Burt, "Load frequency control in variable inertia systems," *IEEE Trans. Power Syst.*, vol. 35, no. 6, pp. 4904-4907, 2020.

[6] P. Hidalgo-Gonzalez, R. Henriquez-Auba, D. S. Callaway and C. J. Tomlin, "Frequency regulation using data-driven controllers in power grids with variable inertia due to renewable energy," *IEEE Power Energy Soc. Gen. Meeting*, Atlanta, GA, USA, 2019, pp. 1-5.

[7] J. C. Willems, "From time series to linear system – Part I. Finite dimensional linear time invariant systems," *Automatica*, vol. 22, no. 5, pp. 561–580, 1986.

[8] C. V. Rao, J. B. Rawlings, J. H. Lee, "Constrained linear state estimation — a moving horizon approach," *Automatica*, vol. 37, pp. 1619-1628, 2001.

[9] T. Liu, D. J. Hill and C. Zhang, "Non-disruptive load-side control for frequency regulation in power systems," *IEEE Trans. Smart Grid.*, vol. 7, no. 4, pp. 2142-2153, 2016.

[10] J. C. Willems, P. Rapisarda, I. Markovsky, and B. L. DeMoor, "A note on persistency of excitation," *Syst. Control Lett.*, vol. 54, no. 4, pp. 325–329, 2005.

[11] C. D. Persis and P. Tesi, "Formulas for data-driven control: stabilization, optimality, and robustness," *IEEE Trans. Autom. Control*, vol. 65, no. 3, pp. 909–924, 2020.

[12] A. Ulbig, T. S. Borsche, and G. Andersson, "Impact of low rotational inertia on power system stability and operation," *IFAC World Congress*, Cape Town, South Africa, 2014.

[13] Y. Zhao, T. Liu and D. J. Hill, "A data-enabled predictive control method for frequency regulation of power systems," *IEEE PES Innov. Smart Grid Technol. Conf. Europe*, Espoo, Finland, 2021, pp. 1-6.

[14] S. Yu, C. Böhm, H. Chen, F. Allgöwer, "Moving horizon l_2 control of LPV systems subject to constraints," *IFAC Proceedings Volumes*, vol 42, issue 13, pp. 354-359, 2009.

[15] H. Atoui, O. Sename, V. Milanés and J. J. Martinez, "LPV-based autonomous vehicle lateral controllers: a comparative analysis," *IEEE Trans. Intell. Transp. Syst.*, vol. 23, no. 8, pp. 13570-13581, 2022.

[16] H. A. Pipino, M. M. Morato, E. Bernardi, E. J. Adam, J. E. Normey-Rico, "Nonlinear temperature regulation of solar collectors with a fast adaptive polytopic LPV MPC formulation," *Solar Energy*, vol 209, pp. 214-225, 2020.

[17] P. M. Ashton, C. S. Saunders, G. A. Taylor, A. M. Carter, and M. E. Bradley, "Inertia estimation of the GB power system using synchrophasor measurements," *IEEE Trans. Power Syst.*, vol. 30, no. 2, pp. 701–709, 2015.

[18] P. Kundur, *Power System Stability and Control*. NY: McGraw-Hill, 1994.

[19] Y. Zhang and C. Peng, "Adaptive $H\infty$ event-triggered load frequency control in islanded microgirds with limited spinning reserve constraints," *Protection and Control of Modern Power Systems*, vol. 8, no. 2, pp. 495-507, 2023.

TABLE III: ISE of different control methods

	AGC	CMPC	SMPC	DAPFC(exact vertices)	DAPFC(inexact vertices)
ISE	304.099	283.559	0.374	0.375	0.378

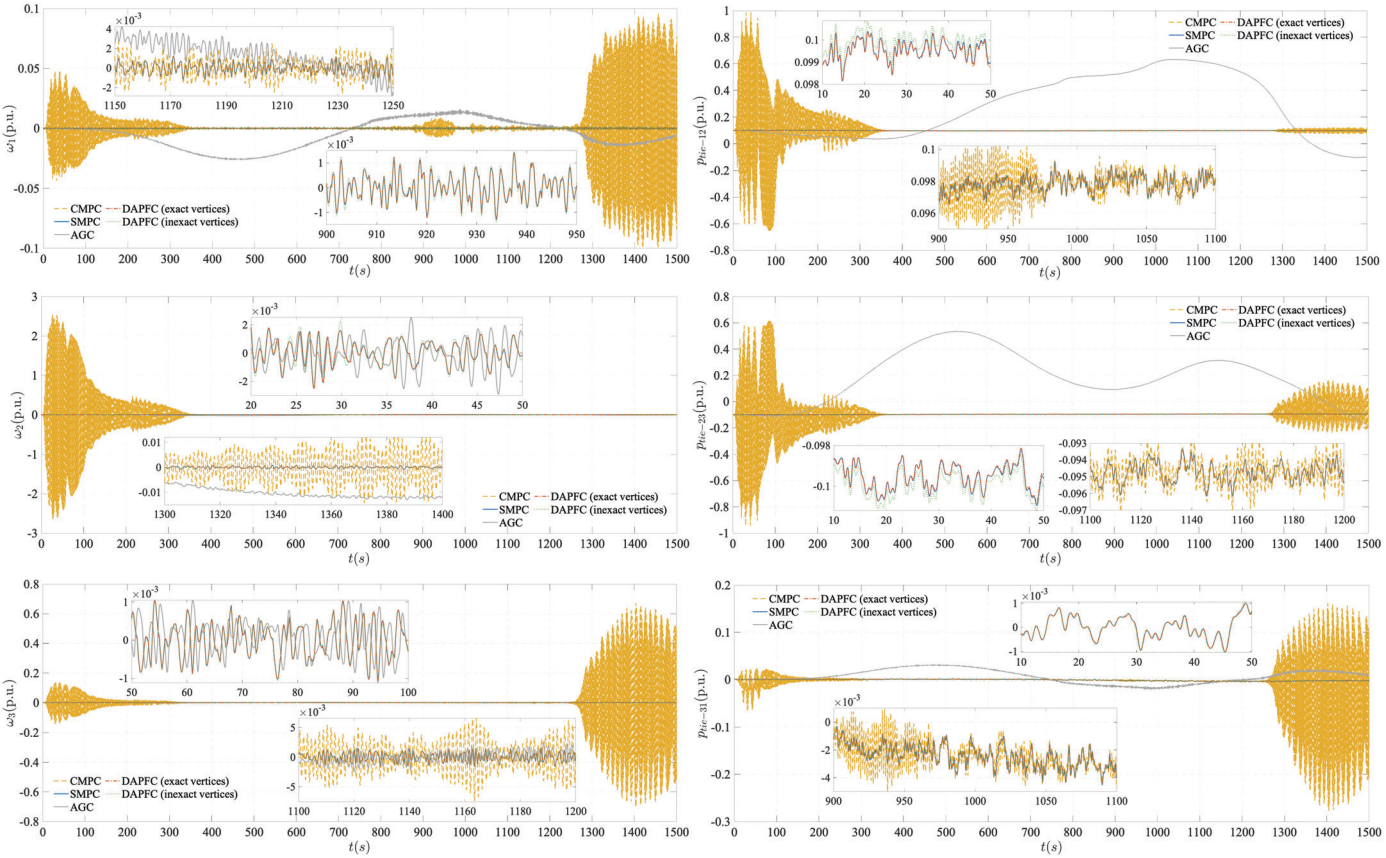

Fig. 5: Control performance of different methods. (left: frequency; right: tie-line power)

[20] W. Kong, Z. Y. Dong, Y. Jia, D. J. Hill, Y. Xu and Y. Zhang, "Short-term residential load forecasting based on LSTM recurrent neural network," *IEEE Trans. Smart Grid*., vol. 10, no. 1, pp. 841-851, 2019.

[21] X. Peng, Y. Chen, K. Cheng, H. Wang, Y. Zhao, B. Wang, J. Che, C. Liu, J. Wen, C. Lu, and W. Lee, "Wind power prediction for wind farm clusters based on the multifeature similarity matching method," *IEEE Trans. on Ind. Appl.*, vol. 56, no. 5, pp. 4679-4688, 2020.